MOLECULAR AND CELLULAR BIOLOGY, Aug. 2011, p. 3286–3297 Vol. 31, No. 16
0270-7306/11/$12.00 doi:10.1128/MCB.01426-10

The Lysyl Oxidase Propeptide Interacts with the Receptor-Type Protein Tyrosine Phosphatase Kappa and Inhibits β-Catenin Transcriptional Activity in Lung Cancer Cells▽

Nuria Sánchez-Morgan,[1] Kathrin H. Kirsch,[2] Philip C. Trackman,[3] and Gail E. Sonenshein[1]*

Department of Biochemistry, Tufts University School of Medicine, Boston, Massachusetts 02111[1]; Department of Biochemistry, Boston University School of Medicine, Boston, Massachusetts 02118[2]; and Division of Oral Biology, Boston University Henry M. Goldman School of Dental Medicine, Boston, Massachusetts 02118[3]

Received 16 December 2010/Returned for modification 8 February 2011/Accepted 6 June 2011

The propeptide region of the lysyl oxidase proenzyme (LOX-PP) has been shown to inhibit Ras signaling in NIH 3T3 and lung cancer cells with activated *RAS*, but its mechanism of action is poorly understood. Here, a yeast two-hybrid assay of LOX-PP-interacting proteins identified a clone encoding the intracellular phosphatase domains of receptor-type protein tyrosine phosphatase kappa (RPTP-κ), and the interaction of the two proteins in mammalian cells was confirmed. RPTP-κ is proteolytically processed to isoforms that have opposing effects on β-catenin activity. The RPTP-κ transmembrane P subunit interacts with and sequesters β-catenin at the cell membrane, where it can associate with E-cadherin and promote intercellular interactions. At high cell density, further processing of the P subunit yields a phosphatase intracellular portion (PIC) subunit, which chaperones β-catenin to the nucleus, where it can function to activate transcription. Lung cancer cells were found to contain higher PIC levels than untransformed lung epithelial cells. In H1299 lung cancer cells, ectopic LOX-PP expression reduced the nuclear levels of PIC by increasing its turnover in the lysosome, thereby decreasing the nuclear levels and transcriptional activity of β-catenin while increasing β-catenin membrane localization. Thus, LOX-PP is shown to negatively regulate pro-oncogenic β-catenin signaling in lung cancer cells.

The enzyme lysyl oxidase (LOX) catalyzes oxidative modifications that promote the formation of lysine-derived covalent cross-links needed for the normal structural integrity of the extracellular matrix. LOX is synthesized as a 50-kDa inactive proenzyme (pro-LOX), which is N- and O-glycosylated within sites of the propeptide domain (45), secreted, and then cleaved to the functional C-terminal ~30-kDa enzyme and an ~18-kDa N-terminal lysyl oxidase propeptide (LOX-PP). Another major function of the *LOX* gene was discovered with the observation that its expression inhibited the transforming activity of the H-*Ras* oncogene in NIH 3T3 fibroblasts (6, 22). Consistent with this finding, many cancers and derived cell lines display reduced levels of LOX protein or RNA (3, 5, 12, 16, 17, 22, 24, 25, 38). LOX reexpression was also seen in stable phenotypic revertants of *Ras*-transfected NIH 3T3 cells following interferon treatment (5, 22). These and other findings led Contente et al. (5) to term the *LOX* gene the *Ras* recision gene (*rrg*). Subsequently, pro-LOX was shown to inhibit the activities of the Akt and Erk kinases and NF-κB transcription factors in *Ras*-transformed NIH 3T3 cells (19), and ectopic expression of the *LOX* gene in gastric cancer cells resulted in reduced tumor formation in nude mice (21). More recently, our group noted that LOX-PP was sufficient to mediate the *rrg* activity of the *LOX* gene in *Ras*-transformed NIH 3T3 cells (35). Consistent with these findings, Bouez et al. showed that LOX protein expression was absent from human basal and squamous cell carcinomas and that a reduction in *LOX* mRNA levels but not enzyme activity caused a more invasive phenotype in a HaCaT skin equivalent model (3). In H1299 lung cancer cells, ectopic LOX-PP expression potently inhibited signaling by the endogenous mutant *NRAS* gene and the ability of these cells to form invasive colonies in Matrigel (46), while in prostate cancer cells, the addition of recombinant LOX-PP (rLOX-PP) protein decreased RAS signaling (45). Similarly, LOX-PP reduced fibronectin-stimulated signaling and the migration of Her-2/neu-driven breast cancer cells (49) and Ras signaling and the ability of pancreatic and breast cancer cells to form tumors in xenograft models in nude mice (30, 31, 46). The mechanisms by which LOX-PP exerts these anticancer effects are only beginning to be understood (see Discussion). Notably, we were unable to detect any evidence for LOX-PP–Ras interaction in a yeast two-hybrid assay (K. H. Kirsch, unpublished observations), indicating that LOX-PP does not appear to exert its anti-Ras signaling effects via direct interaction. Thus, in this study, yeast two-hybrid screening was used to identify proteins that interact with the propeptide, and the receptor-type protein tyrosine phosphatase kappa (RPTP-κ) was newly characterized as a LOX-PP binding partner.

Protein tyrosine phosphatases catalyze the dephosphorylation of phosphotyrosine (p-Tyr) peptides and proteins implicated in signal transduction pathways. RPTP-κ belongs to the family of RPTPs. It has an extracellular region containing a meprin/A5/μ (MAM) domain, an immunoglobulin-like domain, four fibronectin III-like repeats, a transmembrane domain, and two tandem intracellular p-Tyr-specific phosphatase domains (20, 40, 48, 50). RPTP-κ is made as a precursor

* Corresponding author. Mailing address: Tufts University School of Medicine, Department of Biochemistry J808, 150 Harrison Avenue, Boston MA 02111. Phone: (617) 636-4091. Fax: (617) 636-2409. E-mail: gail.sonenshein@tufts.edu.

▽ Published ahead of print on 20 June 2011.

protein that is cleaved by furin to generate two subunits that are noncovalently attached to each other: the ~95-kDa transmembrane P subunit and the 120-kDa extracellular E subunit (2). At high cell densities, RPTP-κ expression increases (9, 11) and the P isoform undergoes proteolytic processing first to an 80-kDa PΔE subunit by ADAM10 and then to an ~70-kDa phosphatase intracellular portion (PIC) subunit by the γ-secretase complex (2). RPTP-κ associates with β-catenin, and its processing has important biological consequences for the bifunctional β-catenin protein, which can be an important component of either adherens junctions or transcriptional coactivators (1, 13).

When β-catenin is localized to the cell membrane as a component of adherens junctions, it links cadherin adhesion receptors to α-catenin, which in turn associates with the cytoskeleton, functioning to stabilize cell adhesion. In the cytoplasm, free β-catenin is targeted for degradation through its association with the adenomatous polyposis coli (APC) and axin proteins, which can recruit glycogen synthase kinase-3β (GSK-3β) and casein kinase I to form a destruction complex that phosphorylates β-catenin, targeting it for proteasome-mediated degradation. Alternatively, inhibition of GSK-3β activity leads to the stabilization of β-catenin, which can then move to the nucleus. Nuclear β-catenin links T cell factor (TCF)/lymphoid enhancer factor (LEF) with other nuclear transcriptional regulators to activate transcription of TCF/LEF-responsive genes, such as c-*MYC*, the epidermal growth factor receptor gene (*EGFR*), and *FRA-1* (18, 28, 44). Understandably, tight regulation of β-catenin activities is necessary to maintain proper tissue architecture and cell fate decisions during normal development. Failure to destroy free cytoplasmic β-catenin promotes colon cancer, non-small cell lung cancer, and other human tumors (1, 10, 29).

The RPTP-κ P and PIC isoforms have been shown to serve opposing roles in the regulation of β-catenin (2). At the cellular membrane, the RPTP-κ P isoform associates with β-catenin and γ-catenin (plakoglobin) (9), two key molecules involved in the formation of cell-cell adhesions, and mediates homophilic intercellular interactions. This association with RPTP-κ stabilizes E-cadherin–β-catenin complexes at cell-to-cell contact regions, decreasing the pool of β-catenin in the cytoplasmic and nuclear compartments (34). In contrast, the PIC isoform functions as an activator of β-catenin transcriptional activity by chaperoning it to the nucleus, possibly by facilitating the dephosphorylation of β-catenin-associated factors for TCF activation (2). In this study, we demonstrate for the first time that LOX-PP interacts with RPTP-κ in lung cancer cells and leads to a decrease in the relative level of the PIC isoform via its degradation in the lysosome. As a consequence, LOX-PP expression in lung cancer cells leads to an overall decrease in β-catenin nuclear levels and transcriptional activity, an increased accumulation of β-catenin at the plasma membrane, and a less-transformed lung cancer cell phenotype.

MATERIALS AND METHODS

Cell lines and culture conditions. Human H1299, H1729, and A549 lung cancer cells were kindly provided by Zhi-Xiong Jim Xiao (Boston University School of Medicine, Boston, MA). Human H23 and Calu-1 lung cancer cells were generously provided by Hasmeena Kathuria (Boston University School of Medicine). The spontaneously immortalized adult murine lung epithelial cell line E10 was kindly provided by Alvin Malkinson (University of Colorado Cancer Center, Aurora, CO). Lung cell lines and human embryonic kidney (HEK) 293T cells were grown as specified by the American Type Culture Collection (Manassas, VA). H1299 clones with LOX-PP in the doxycycline (Dox)-inducible pCXR(TO) vector or empty vector (EV) control (see below) were established by transfection with the regulator vector pTRE and either pCXR(TO)-LOX-PP or the control pCXR(TO) parental (EV) vector. Transfected cells were selected with 10 μg/ml blasticidin (Invitrogen, Carlsbad, CA) and 600 μg/ml Geneticin (Sigma, St. Louis, MO). Single clones of cells expressing LOX-PP were isolated by limiting dilution, and LOX-PP expression confirmed. To test for the effects of LOX-PP on EGF receptor (EGFR) activation, A549 cells in 100-mm dishes were transiently transfected with 5 μg of EV or LOX-PP expression vector using Fugene 9 (Roche Diagnostics, Indianapolis, IN) according to the manufacturer's directions. After 24 h, cultures were incubated overnight in medium containing 0.5% fetal bovine serum (FBS) and stimulated with 100 ng/ml EGF (product number E9644; Sigma) for 15 min, and whole-cell extracts prepared.

Antibodies. The RPTP-κ antibody (RPTP-κJM) was kindly provided by Axel Ullrich (Max Planck Institute of Biochemistry, Martinsried, Germany). The following antibodies were from Santa Cruz Biotechnology (Santa Cruz, CA): lamin B (sc6217), c-MYC (9E10), EGFR (sc-1005), Fra-1 (sc-183), and normal rabbit IgG (sc-2027). The β-catenin (610153) and β-actin (AC-15) antibodies were from BD Transduction (Franklin Lakes, NJ) and Sigma, respectively. The phospho-EGFR antibody (2234) was from Cell Signaling (Danvers, MA). The LOX-PP antibody (NBP1-30327) was from Novus (Littleton, CO). The following antibodies were from Invitrogen: secondary anti-mouse IgG–Alexa Fluor 594 (catalog number A21201), secondary anti-mouse IgG–Alexa Fluor 555 (catalog number A21422), anti-green fluorescent protein (anti-GFP) (catalog number A-6455), and anti-V5 (catalog number R960-25).

Constructs. The human propeptide region of lysyl oxidase (minus the signal peptide [SP]) was amplified from placenta cDNA using PCR with forward primer 5′-CACGAATTCCCTCCCGCCGCCGGCCAA-3′ and reverse primer 5′-GTCG TCGCGTCGACAGCCGTCCACGCGGCTGGGGGGCCGCAGGTTACT-3′. The amplified cDNA was cloned in frame into the EcoRI and SalI sites of the yeast expression vector pGBKT7. A mammalian expression construct for the human lysyl oxidase propeptide fused in frame with a V5 epitope tag at the C terminus was constructed by PCR amplification using the following primers: 5′-ATGGCCATGG AGGGATCCATGCCTCCCGCCGCCGGCCAA-3′ and 5′-AGGGTCGTCGCT CGAGATGCCGTCCACGCGGCT-3′. The amplified cDNA was cloned into the BamHI and XhoI sites of the pcDNA6/V5-HisB vector (Invitrogen). A mammalian expression construct for the human lysyl oxidase propeptide minus the SP (amino acids 23 to 124) fused in frame with the GFP at the C terminus was constructed using PCR with the following primers: 5′-ACCGAGCTCGGGAATTCGCCTCCCGCC GCCGGCCAA-3′ and 5′-CGGGCCCTCTAGACTGGATCCGCCGTCCACGC GGCT-3′. The amplified cDNA was cloned into the BamHI and EcoRI sites of the pEGFPC1 expression vector (Clontech, Mountain View, CA). A mammalian expression construct for the phosphatase domains of RPTP-κ fused in frame with GFP at the C terminus was constructed by using PCR with the following primers: 5′-CA ACCTCGAGAGATGGATCCTTCCTCAGA-3′ and 5′-CTCACCGGATCCAGA TGAATTCCAGGTACTC-3′. The amplified cDNA was cloned into the BamHI and XhoI sites of the pEGFPC1 expression vector (Clontech). An inducible expression system for LOX-PP containing a C-terminal V5-His tag was created by excision of the human LOX-PP cDNA from the pcDNA4-V5/His vector and subcloning of the fragment into the PmeI site of the retroviral vector pCXR(TO) containing a Dox-inducible promoter or into vector pCX_{bsr} under the control of a constitutive cytomegalovirus immediate-early promoter (generously provided by T. Akagi, OBI, Osaka, Japan). The integrity of all of the constructs synthesized was confirmed by restriction enzyme digestion and DNA sequencing. Mammalian expression constructs for RPTP-κ and its PIC isoform fused in frame with a hemagglutinin (HA) tag were kindly provided by Axel Ullrich (2). The pTOP and pFOP TCF reporter plasmids were kindly provided by Isabel Domínguez (Boston University School of Medicine).

Yeast two-hybrid library screening. The AH109 yeast strain, which carries the *HIS3*, *ADE2*, *LEU2*, and *lacZ* reporter genes under the regulatory control of GAL4, was propagated in yeast-peptone-dextrose (YPD) medium (catalog number 8600-1), YPD agar medium (catalog number 8601-1), minimal synthetic defined (SD) base (catalog number 8602-1), or minimal SD agar base (catalog number 8603-1) (all from Clontech), as required. For the two-hybrid screen, AH109 yeast cells stably expressing LOX-PP in the pGBKT7 backbone were transformed with a human breast cancer cDNA library cloned in pGAD10 (pGAD10 carries the *LEU2* gene as selectable marker) (catalog number HL4036AH; Clontech) using Yeastmaker transformation system 2 (catalog number 630 439; Clontech). Double transformants were grown on yeast plates lacking leucine (Leu) and tryptophan (Trp) (−Leu/−Trp) or Leu, Trp, and histidine

(His) (−Leu/−Trp/−His). Growth in the −Leu/−Trp/−His triple selection plates was conferred by an interaction of LOX-PP with the protein expressed by the library plasmid. Identified novel associations were confirmed using a β-galactosidase colony-lift filter assay as described previously (32). Library plasmids from confirmed interactions were isolated and sequenced, and putative LOX-PP-interacting proteins were identified by performing computer searches of nucleic acid and protein databases to determine homologies of the isolated clones with previously identified proteins.

Luciferase reporter assays. H1299 cells growing in 6-well plates were transfected with pTOP or pFOP TCF luciferase reporter plasmids (0.5 μg) and empty vector ($pcDNA_4$, 1.0 μg) or a LOX-PP expression plasmid (pcLOX-PP, 1.0 μg) using Fugene 6 (Roche Diagnostics). All samples were normalized for transfection efficiency using a *Renilla* expression plasmid (10 ng) (Promega, Madison, WI) as an internal control. Cells were incubated at 37°C and harvested at 48 h posttransfection. Luciferase activity was assayed using a Dual-Luciferase reporter assay system (catalog number E1910; Promega). Transfections were performed in triplicate and repeated three times.

Immunoprecipitation and immunoblot analysis. LOX-PP was immunoprecipitated from medium supernatants as described previously (27). Briefly, 1 ml of culture medium was subjected to immunoprecipitation using a V5 or LOX-PP antibody, as appropriate. Immunocomplexes were isolated as described below for immunoprecipitation analysis and subjected to immunoblot analysis. For coimmunoprecipitation of LOX-PP and RPTP-κ, HEK 293T cells were plated in 100-mm dishes and transfected with 3 μg each of vectors expressing GFP (control) and HA-RPTP-κ or GFP-LOX-PP and HA-RPTP-κ using Fugene 6. Cells were incubated at 37°C for 48 h, washed in cold phosphate-buffered saline (PBS), and lysed in Triton X-100 lysis buffer, as described previously (2). Cell lysates (200 μg) were incubated with either an antibody against RPTP-κ, GFP, or a control goat IgG or rabbit IgG on a rocker platform overnight at 4°C. Protein A/G-plus-agarose beads (catalog number sc-2003; Santa Cruz Biotechnology) were then added, and the incubation continued for 2 h at 4°C. Beads were then collected by centrifugation, washed three times in PBS, and resuspended in SDS loading dye and the eluted proteins subjected to immunoblotting.

Whole-cell extracts and nuclear and cytoplasmic fractions were prepared as described previously (30, 46). Triton X-100-insoluble fractions were prepared as described previously (37). Protein concentrations were determined using a detergent-compatible protein assay kit (Bio-Rad, Hercules, CA) and samples (50 μg) were subjected to immunoblotting as described previously (30). Molecular mass markers (product number 161-0318; Bio-Rad) were used on each gel.

Immunofluorescence microscopy. H1299 control (EV) or LOX-PP-expressing clone 3, 5, or 8 was plated on coverslips. Following induction with 2 μg/ml of doxycycline or an equal volume of water vehicle control for 48 h at 37°C, cells were washed with PBS, incubated in fixative solution (2% electron microscopy-grade paraformaldehyde [EMS, Hatfield, PA], PBS, 5 mM $MgCl_2$) for 15 min, rinsed in PBS, and stored in 70% ethanol at 4°C until use. Alternatively, 2×10^5 H1299 cells were plated on coverslips in 6-well dishes and transfected with 0.5 μg of a GFP-tagged PIC expression construct (GFP-PIC) and either 0.5 μg of a V5-tagged LOX-PP expression construct or EV as a negative control using Fugene 6. Cells were incubated overnight at 37°C and fixed as described above. For immunofluorescence analysis, cells were rehydrated in PBS and permeabilized with 0.2% Triton X-100 in PBS. Cells were subsequently washed in PBS, blocked by incubation in buffer A (2% [wt/vol] bovine serum albumin [Sigma] in PBS), and incubated for 1 h in primary antibody diluted in buffer A. Following washing, the coverslips were incubated for 1 h in Alexa Fluor-labeled secondary antibodies diluted in buffer A. The coverslips were washed and mounted in Vectashield with 4′,6-diamidino-2-phenylindole (DAPI) (catalog number H-1200; Vector Laboratories, Burlingame, CA). Fluorescence microscopy was performed using either a Zeiss Axiovert 200 M microscope with a 40× objective or a Nikon Eclipse E400 with a 100× objective. The images in the figures are representative of two independent experiments done in duplicate.

Migration assay. Control H1299 cells (EV) or LOX-PP-expressing cells (clones 3, 5, and 8) were induced with 2 μg/ml of Dox for 24 h. Suspensions of 1×10^5 cells were plated in the upper chamber of a Transwell (Costar, Cambridge, MA) dish on an 8-mm-diameter polycarbonate filter (8-μm pore size) and incubated at 37°C for 5 h. Migration of cells to the lower side of the filter was measured with an acid phosphatase enzymatic assay using *p*-nitrophenyl phosphate as a substrate and determination of the optical density at 410 nm. Assays were performed 3 independent times, each in triplicate, and significance was determined using Student's *t* test.

Colony formation assay. Control H1299 cells (EV) or LOX-PP-expressing cells (clones 3, 5, and 8) were plated at 100 cells/well in 6-well plates, induced with 2 μg/ml of Dox, and incubated at 37°C. Seven days later, when colonies were visible, cells were washed twice with PBS, fixed with methanol, and stained with

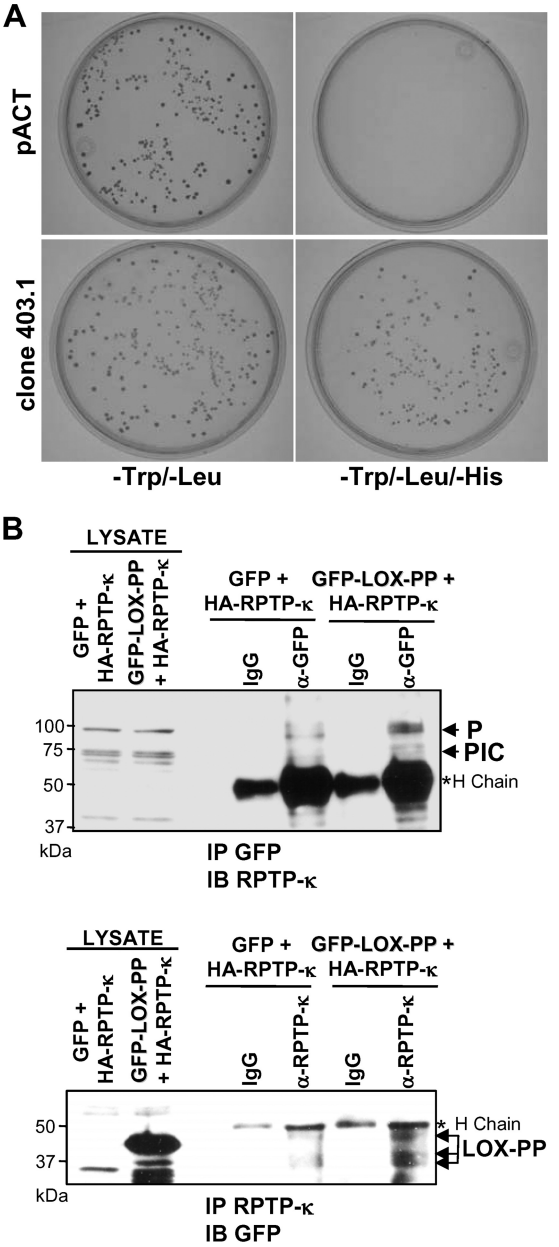

FIG. 1. LOX-PP interacts with RPTP-κ in yeast and mammalian cells. (A) Yeast AH109 cells expressing LOX-PP were transformed with an empty library vector (pACT) or the RPTP-κ library clone 403.1. Transformants were plated in minimal medium (−Trp/−Leu or −Trp/−Leu/−His) to probe for expression of the reporter genes. (B) HEK 293T cells were transfected with an HA-tagged RPTP-κ expression plasmid (3 μg) in combination with 3 μg of vectors expressing either GFP (control) or GFP-LOX-PP. After 48 h, whole-cell lysates (200 μg) were subjected to immunoprecipitation with an antibody directed against either GFP (α-GFP, upper panel) or RPTP-κ protein (α-RPTP-κ, lower panel) or control IgG (IgG). The immunoprecipitated (IP) proteins and samples of lysates were separated by SDS-PAGE. The resulting immunoblots (IB) were analyzed using an antibody against RPTP-κ (IP GFP, IB RPTP-κ, upper panel) or GFP (IP RPTP-κ, IB GFP, lower panel). Positions of the precipitated ~95-kDa P subunit, ~70-kDa PIC subunit, and LOX-PP proteins are indicated. For estimation of the amounts of expressed proteins, 17% of each of the lysates was separated and immunoblotted (LYSATE lanes).*H chain, immunoglobulin heavy chain. The positions of molecular mass markers are given on the left.

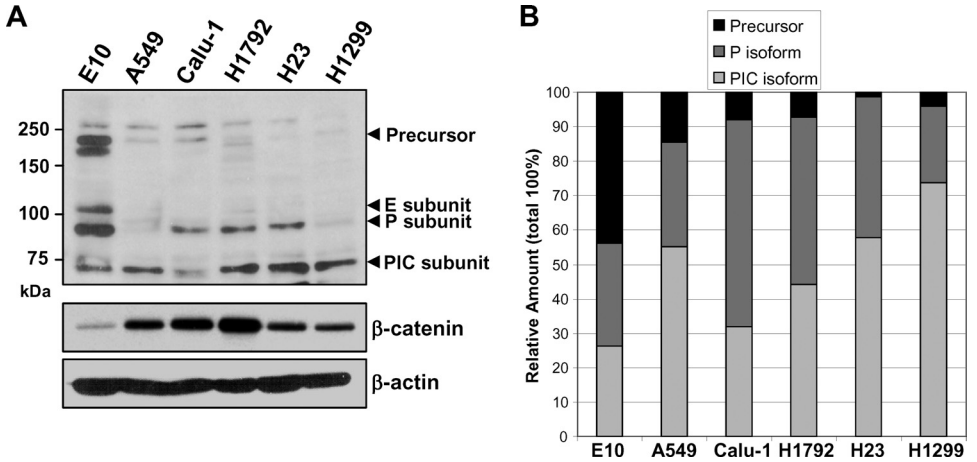

FIG. 2. RPTP-κ is differentially expressed in lung epithelial and cancer cell lines. (A) Whole-cell extracts were isolated from cultures of the indicated spontaneously immortalized mouse lung epithelial or human lung cancer cell lines at 85 to 90% confluence and analyzed by immunoblotting for RPTP-κ and β-catenin and for β-actin, which confirmed essentially equal loading. (B) The Western blot shown in panel A and two additional duplicate blots were subjected to densitometry, and the percentages of the various subunits present in each cell line are represented.

toluidine blue (Sigma). Scion Image analysis software was used to determine the number of colonies per well.

RNA knockdown analysis. The following RNA duplexes used for targeting human *LOX* were purchased from Qiagen (Gaithersburg, MD; GS4015): oligonucleotide 1, 5′-CTGCACAATTTCACCGTATTA-3′ (product number S100036113), and oligonucleotide 2, 5′-AAGCTGGCTACTCGACATCTA-3′ (product number S100036120). The small interfering RNAs (siRNAs) were transfected at a final total concentration of 20 nM using Lipofectamine RNAiMax (Invitrogen). The negative-control siRNA used was from Qiagen (product number 1027310). After 48 h, medium was collected and whole-cell extracts prepared and subjected to immunoblotting analysis as described above.

Real-time PCR analysis. H1299 control or LOX-PP-expressing clones 3 and 5 were incubated for 48 h with doxycycline. RNA was prepared using a NucleoSpin RNAII kit (Macherey-Nagel, Bethlehem, PA) and quantified by measuring the A_{260}. To prepare cDNA, 1 μg of RNA was reverse transcribed with Superscript RNase H-RT in the presence of 100 ng of random primers (Invitrogen). Real-time PCR was performed three times in triplicate using a Roche Light Cycler 480II with 96-well plates and SYBR green mix (Roche Diagnostics). The threshold values for each gene were normalized to the expression levels of glyceraldehyde-3-phosphate dehydrogenase (GAPDH). The forward (F) and reverse (R) primers used were as follows: GAPDH-F, 5′-TTGCCATCAATGACCCCTTCA-3′; GAPDH-R, 5′-CGCCCCACTTGATTTTGGA-3′; c-MYC-F, 5′-TCAAGAGGCGAACACACAAC-3′; c-MYC-R, 5′-GGCCTTTTCATTGTTTTCCA-3′; EGFR-F, 5′-CGCAAGTGTAAGAAGTGCGAA-3′; EGFR-R, 5′-CGTAGCATTTATGGAGAGTGAGTCT-3′; FRA-1-F, 5′-CGAAGGCCTTGTGAACAGAT-3′; and FRA-1-R, 5′-CTGCAGCCCAGATTTCTCAT-3′.

RESULTS

Two-hybrid screening identifies RPTP-κ as a LOX-PP binding protein. To identify cellular binding partners that mediate the *rrg* activity of LOX-PP, yeast two-hybrid screening was performed. The screen was made with a human breast cancer cDNA library and a bait construct consisting of LOX-PP minus the signal peptide region. The integrity of the construct, the expression of LOX-PP in AH109 yeast cells, and the absence of autonomous LOX-PP DNA-binding ability were confirmed (data not shown). The cDNA library was transformed into AH109 yeast cells containing a LOX-PP expression construct (pGBKT7-LOX-PP). Five hundred seventy-five clones were isolated. These clones were further analyzed using a filter β-galactosidase assay to confirm the positive interactions identified. A total of 405 clones were confirmed. Positive colonies from this second screen were replated and amplified in minimal medium lacking tryptophan to allow for the loss of the LOX-PP expression vector. Library plasmids were subsequently isolated, and 96 target cDNAs were subjected to DNA sequencing. Putative LOX-PP-interacting proteins were identified by performing computer searches of nucleic acid and protein databases to determine the homologies of the isolated clones with previously identified proteins. Clones expressing identified proteins were grouped into categories according to their cellular location/function. Of note, in the screen, we isolated clones coding for the α1 and α2 chains of type I collagen and the α1 chain of type III collagen, which are substrates of LOX enzyme activity, and for fibronectin, which has been reported to interact with the LOX enzyme (8). One clone encoded the intracellular catalytic phosphatase domains of RPTP-κ, which is a class II transmembrane phosphatase. As receptor tyrosine kinases signal via Ras, RPTP-κ was of particular interest.

RPTP-κ interacts with LOX-PP in yeast and mammalian cells. We next sought to confirm the interaction of RPTP-κ with LOX-PP. Yeast cells expressing LOX-PP were transformed with empty vector (pACT) or the library cDNA clone for RPTP-κ (clone 403.1) and plated on nutritional dropout plates to test for reporter gene expression. As shown in Fig. 1A, RPTP-κ was able to activate the expression of the *HIS* reporter gene in yeast cells expressing LOX-PP, but the empty pACT vector control did not activate it. This result was confirmed by a β-galactosidase filter assay (data not shown).

To confirm that the interaction between RPTP-κ and LOX-PP occurs in mammalian cells, coimmunoprecipitation analysis was performed. HEK 293T cells were transfected with vectors expressing an HA-tagged RPTP-κ (HA-RPTP-κ) in the presence of either an expression construct for LOX-PP fused to GFP at its amino terminus (GFP-LOX-PP) or for GFP alone, as a control. Extracts were immunoprecipitated with an antibody against GFP and immunoblotted for RPTP-κ using an antibody raised against the cytoplasmic juxtamembrane region of RPTP-κ that can detect the ~95-kDa P, 80-

kDa PΔE, and ~70-kDa PIC isoforms (2). Immunoprecipitation of GFP-tagged LOX-PP was found to robustly bring down the P subunit of RPTP-κ, while coprecipitation of the PIC isoform was relatively much more modest (Fig. 1B, upper panels). Since both contain the phosphatase domains, these results suggest the possibility of differential interaction or that the association with LOX-PP alters the stability and/or processing of RPTP-κ (see below). Conversely, extracts were immunoprecipitated with an antibody against RPTP-κ and immunoblotted for GFP. Full-length as well as what may be either clipped or processed GFP-LOX-PP was detected in complexes immunoprecipitated with an RPTP-κ antibody (Fig. 1B, lower panels). Thus, LOX-PP was associated with the ~95-kDa P subunit and the ~70-kDa PIC isoform of RPTP-κ in HEK 293T cells.

RPTP-κ is highly expressed in lung cancer cells. RPTP-κ has been reported to be highly expressed in the human lung (9). The levels of RPTP-κ isoforms were assessed in whole-cell extracts of the untransformed murine E10 lung epithelial cell line and of five human lung cancer cell lines. Expression of the ~95-kDa RPTP-κ P transmembrane and ~70-kDa PIC isoforms of RPTP-κ was detected in all of the lines (Fig. 2A), although the ratios varied considerably. Of note, the spontaneously immortalized E10 lung epithelial cell line contained a very high relative level of the full-length RPTP-κ and the P subunit, consistent with its more normal phenotype (Fig. 2B). Interestingly, the highly metastatic H1299 and A549 lung cancer cells contained the lowest levels of the β-catenin-inhibitory RPTP-κ P isoform and relatively high levels of the PIC subunit, the β-catenin-activating form (Fig. 2B). Thus, the spontaneously transformed line and the cancer lines have differing expression patterns of the various RPTP-κ isoforms, which are expressed at high levels in all of the lung epithelial and cancer cell lines examined.

LOX-PP increases levels of the RPTP-κ P subunit and decreases levels of the PIC isoform in the nucleus. To test for the effects of LOX-PP expression on the levels of the different RPTP-κ isoforms in lung cancer, we used the H1299 lung cancer cell line, which we showed previously is susceptible to LOX-PP treatment (46). Mixed populations of cells were isolated with the parental Dox-inducible pCXR(TO) empty vector (EV) DNA or with the LOX-PP-expressing vector by selection with 600 μg/ml Geneticin and 10 μg/ml blasticidin. As some leakiness in the expression of LOX-PP was observed previously with these cells (46), individual clones expressing LOX-PP (clones 1, 3, 5, and 8) or control clones containing EV DNA were isolated by limiting dilution. To test for the expression of LOX-PP, cultures of LOX-PP clones 3 and 5 or H1299 control EV cells were incubated in the absence or presence of 2 μg/ml Dox for 48 h and the culture medium was collected and probed for LOX-PP secretion (Fig. 3A). Dox treatment induced the expression of LOX-PP in clones 3 and 5 (Fig. 3A). Consistent with the results of previous studies (30, 45), secreted LOX-PP appeared as a glycosylated protein yielding multiple higher-molecular-mass bands (Fig. 3A). As a test of LOX-PP function, we assessed the effect of the induction of LOX-PP on colony formation (Fig. 3B). LOX-PP-expressing clones 3 and 5 displayed substantially decreased colony numbers, consistent with our previous findings (46). Some inhibition was seen in the absence of Dox treatment, consistent with some vector leakiness, but the extent was significantly increased with Dox treatment. Furthermore, the ability of LOX-PP to reduce migration by H1299 lung cancer cells was confirmed (Fig. 3C) (46).

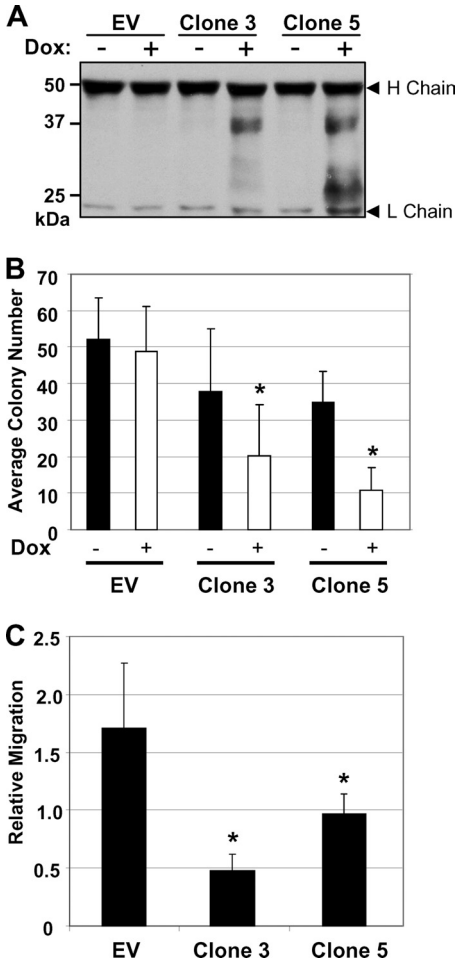

FIG. 3. Effects of ectopic inducible LOX-PP expression on colony formation and migration of H1299 lung cancer cells. (A) H1299 control (EV) clone or LOX-PP-expressing clones 3 and 5 were incubated in the absence (−) or presence (+) of 2 μg/ml of Dox. After 48 h, LOX-PP was immunoprecipitated from 1 ml of cell medium using an antibody specific for the V5 tag. Immunocomplexes were resolved by SDS-PAGE and subjected to immunoblotting for LOX-PP by using a V5 antibody. H chain and L chain, immunoglobulin heavy and light chain, respectively. (B) H1299 control (EV) and LOX-PP-expressing clones 3 and 5 were plated at 100 cells/well in 6-well plates and induced with Dox. Seven days later, cells were washed, fixed with methanol, and stained with toluidine blue. Pictures of individual wells were taken, and Scion Image analysis software was used to determine the number of colonies per well. The assay was repeated three times in triplicate, and results are presented with plus-minus standard deviations. Significance was determined using Student's *t* test. *, $P < 0.05$. (C) H1299 EV and clones 3 and 5 were treated with Dox for 24 h and subjected to a migration assay, in triplicate, for 5 h. Cells that migrated to the lower side of the filter were quantified by spectrometric determination of the optical density at 410 nm. The assay was repeated three times, and results are presented with plus-minus standard deviations. Significance was determined using Student's *t* test. *, *P* values for clones 3 and 5 were 0.01 and 0.038, respectively.

We next used clones 3, 5, and 8 to test for the effects of the induction of LOX-PP on the levels of the different RPTP-κ

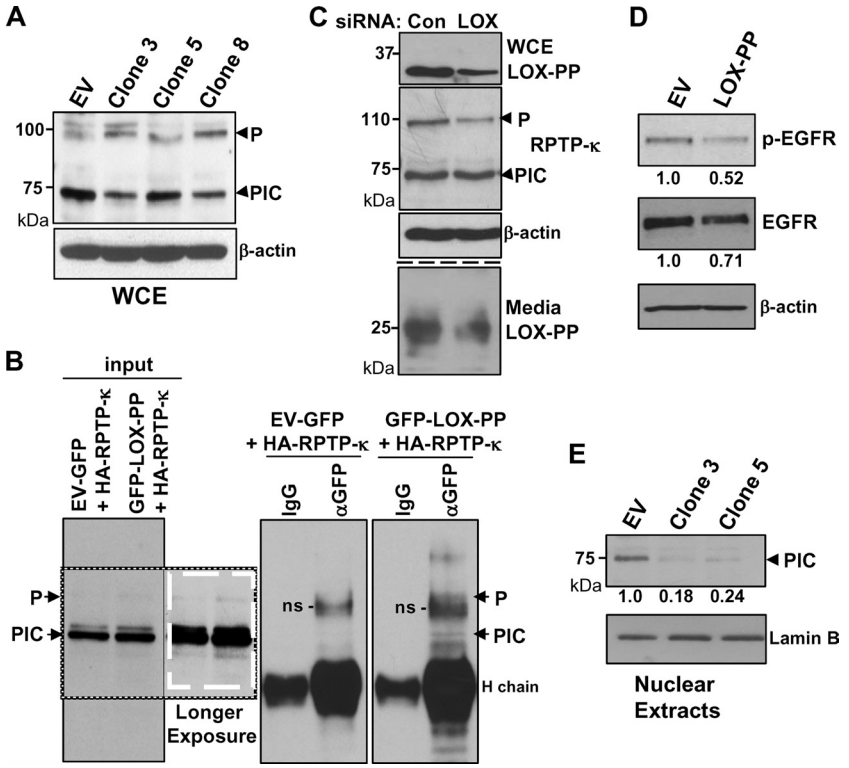

FIG. 4. LOX-PP expression induces changes in the levels and distribution of RPTP-κ isoforms in H1299 cells. (A) Control (EV) or LOX-PP-expressing clones 3, 5, and 8 were incubated in the presence of Dox for 48 h. Whole-cell extracts (WCE) were prepared in RIPA buffer and subjected to immunoblotting for RPTP-κ and β-actin, as a loading control. (B) H1299 cells were transfected with an HA-tagged RPTP-κ expression plasmid (3 μg) in combination with 3 μg of vector expressing either GFP (control) or GFP-LOX-PP. After 48 h, whole-cell lysates were prepared. Following removal of samples for input lanes (17%), the lysates were subjected to immunoprecipitation with an antibody directed against either GFP (αGFP) or control IgG (IgG) and immunoprecipitated proteins analyzed by Western blotting for RPTP-κ. Please note that the lanes are all from the same gel/blot but cut to align in the correct order. A darker exposure of a section of the input lanes is shown, in a white box, to better visualize the P subunit. Positions of the precipitated P subunit and PIC isoform are as indicated. H chain, immunoglobulin heavy chain; ns, nonspecific band. (C) H1299 cells were incubated with either 20 nM control siRNA (Con) or 10 nM (each) LOX siRNAs 1 and 2 (LOX) using Lipofectamine RNAiMax. After 48 h, medium was collected and whole-cell extracts prepared. Intracellular expression of LOX-PP, RPTP-κ, and β-actin (upper panels) and extracellular LOX-PP levels (lower panels) were monitored as described in the Fig. 3 legend except that the Novus anti-human LOX-PP antibody was used. (D) A549 cells were transiently transfected with EV DNA or LOX-PP expression vector. After 24 h, cultures were incubated overnight in medium containing 0.5% FBS and stimulated with 100 ng/ml EGF for 15 min, and whole-cell extracts subjected to Western blotting for p-EGFR, EGFR, and β-actin. The levels of p-EGFR and EGFR in this and one independent replicate experiment were quantified. The average values normalized to the results for the β-actin loading control from the two experiments are given below, relative to the results for control EV DNA (set to 1.0). (E) Control (EV) or LOX-PP clones 3 and 5 were induced with Dox for 48 h. The nuclear fraction was prepared and subjected to immunoblotting for RPTP-κ and for lamin B as a loading control. The results from three independent experiments were subjected to densitometry and normalized to the result for the lamin B loading control, and the mean values relative to the results for control EV cells (set to 1.0) are given.

isoforms. Cultures were treated for 48 h with Dox, and whole-cell extracts were prepared in radioimmunoprecipitation assay (RIPA) buffer and subjected to immunoblotting. In the three LOX-PP-expressing clones, a substantially lower relative level of the PIC isoform was seen, whereas the amount of the P subunit was slightly higher than in the H1299-EV control cells (Fig. 4A). To confirm the interaction of RPTP-κ with LOX-PP in these lung cancer cells, coimmunoprecipitation analysis was performed following cotransfection of H1299 cells with vectors expressing HA-tagged RPTP-κ in the presence of either the GFP-LOX-PP expression construct or GFP alone, as a control (Fig. 4B). Coprecipitation was detected. LOX-PP brought down the P subunit and a potential processing intermediate form that migrated at 155 to 165 kDa. While the PIC isoform was present at a more abundant level than the P subunit in the input lanes (see darker exposure input lanes in Fig. 4B [white box] to visualize the P subunit), very little was seen in the material that coprecipitated with LOX-PP, similar to the findings described above for HEK 293T cells (Fig. 1B). To further test the effects of LOX-PP on P subunit levels, a knockdown strategy was employed. H1299 cells were transfected with a combination of two siRNAs specific for the *LOX* gene or an equal amount of a control siRNA. LOX-PP expression both in the cell layer (Fig. 4C, upper panel) and in the medium (Fig. 4C, lower panel) was substantially reduced, confirming the effectiveness of the human siRNAs. Notably, a decrease in P subunit levels was seen with LOX-PP knockdown (Fig. 4C, middle panels). Together, these results indicate that LOX-PP increases the levels of the P subunit.

Xu et al. have shown that RPTP-κ inhibits EGFR activity, as judged by phosphorylation (47). Analysis of EGFR activity is technically difficult in lung cancer cells due to extremely low

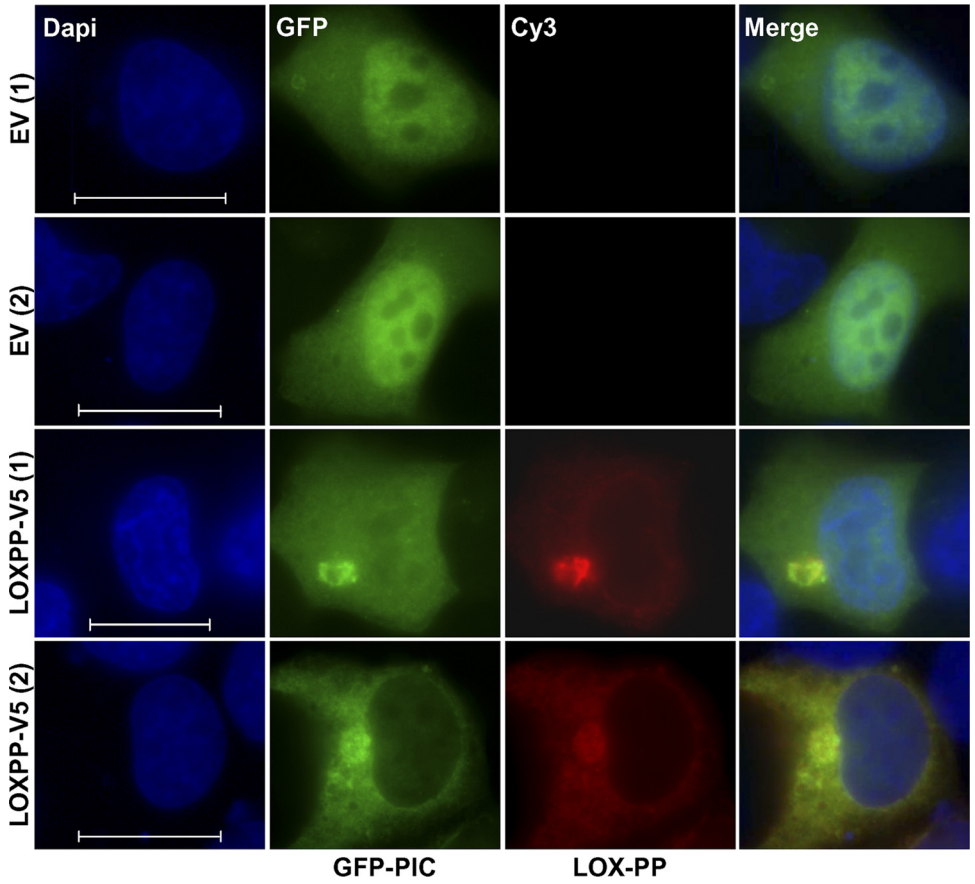

FIG. 5. LOX-PP reduces the nuclear levels of the PIC isoform in lung cancer cells. H1299 cells were cotransfected with GFP-PIC and a V5-tagged LOX-PP construct or EV DNA as a control. For LOX-PP staining, a V5 antibody and anti-mouse Alexa Fluor 555-IgG secondary antibody (red) were used. Nuclei were labeled with DAPI (blue). Fluorescence microscopy was performed using a Nikon Eclipse E400 microscope and a 100× objective. Individual and merged images are shown. Bars = 60 μm.

levels of EGFR. Thus, we sought to determine whether LOX-PP can inhibit the activation of EGFR following stimulation with 100 ng/ml EGF for 15 min. We selected A549 cells since, in our initial analysis, they displayed a higher level of EGFR and p-EGFR could be readily detected after 15 min of EGF stimulation (data not shown). As seen by the results in Fig. 4D, ectopic LOX-PP substantially decreased the activation of p-EGFR induced by EGF stimulation in these cells. The data from this and a second independent experiment were scanned, and the results indicate that LOX-PP reduced the levels of p-EGFR by approximately 50%. Thus, consistent with increasing the levels of the RPTP-κ P subunit, LOX-PP leads to enhanced phosphatase activity in these lung cancer cells.

As PIC chaperones β-catenin to the nucleus, we next asked whether the amount of PIC in the nucleus was affected by LOX-PP. The EV control and LOX-PP-expressing clones 3 and 5 were induced with Dox. After 24 h, nuclear extracts were prepared and subjected to immunoblotting (Fig. 4E). A decreased level of PIC was detected in the nuclei of LOX-PP-expressing clones. The data from three independent experiments were scanned, and the results indicate that nuclear levels of PIC were reduced by ~75 to 80% in comparison to the levels in the EV DNA samples (Fig. 4E). Together, these findings led us to postulate that LOX-PP may be causing relocalization and/or degradation of the PIC isoform.

To more directly assess the effects of LOX-PP on PIC levels in the nucleus, cotransfection analysis was performed using a vector that expresses GFP-tagged PIC protein or GFP alone and either a V5-tagged LOX-PP construct or EV DNA as a control. When H1299 cells were cotransfected with control EV DNA, GFP-PIC showed preferential localization to the nucleus (Fig. 5), as reported previously (2), whereas GFP alone localized throughout the cell, as reported previously (41) (not shown). When cotransfected with LOX-PP, GFP-PIC displayed a reduced nuclear accumulation which ranged from a marked decrease to an almost complete exclusion [see examples LOX-PP-V5 (1) and LOX-PP-V5 (2), respectively, in Fig. 5], consistent with the decreased nuclear PIC levels observed in clones 3 and 5 by Western blot analysis (Fig. 4E). Overall, these results indicate that LOX-PP increases the level of the P subunit of RPTP-κ, which has been shown to relocalize β-catenin to the cell membrane, and decreases the levels of the RPTP-κ PIC subunit, which facilitates β-catenin movement to the nucleus (2, 34).

LOX-PP promotes PIC subunit degradation in the lysosome. Immunofluorescence analysis of LOX-PP distribution in

the H1299 cell line indicated its localization in several sites, including the lysosome and Golgi complex (data not shown). The decreased levels and new localization of PIC in the presence of LOX-PP led us to question whether the propeptide induces a relocalization of PIC to the lysosome, where it is turned over more rapidly. As an initial test, we performed immunofluorescence localization studies to determine whether PIC was present in the lysosome in the presence of LOX-PP. We detected colocalization of GFP-PIC with lysosomal membrane protein 2 (LAMP2) in cells expressing LOX-PP (Fig. 6A). To test whether degradation of PIC was mediated by lysosomal enzymes, H1299 cells were transfected overnight with vectors expressing GFP-PIC with either LOX-PP or EV DNA and treated with the lysosomal inhibitor NH_4Cl. After 4 h, whole-cell extracts were prepared. The decrease in the level of PIC protein seen with LOX-PP was prevented by the addition of NH_4Cl (Fig. 6B). As a positive control for the effects of NH_4Cl on the lysosome, we confirmed its ability to prevent the decrease in the level of EGFR, a lysosomal enzyme-mediated degradation target (Fig. 6B). Consistently, in the presence of NH_4Cl, GFP-PIC again localized predominantly to the nucleus (data not shown). These data suggest that the interaction of PIC with LOX-PP results in lysosomal enzyme-mediated degradation of PIC, leading us to hypothesize that LOX-PP decreases the nuclear levels of β-catenin.

LOX-PP enhances β-catenin localization to the plasma membrane of H1299 lung cancer cells. As an initial test of this hypothesis, control H1299-EV and clone 3, 5, and 8 cells were treated with Dox and the Triton X-100-insoluble fraction isolated and subjected to immunoblotting for β-catenin (Fig. 7A). An increase in the levels of β-catenin in the Triton X-100-insoluble membrane fraction was observed in all three clones. Indirect immunofluorescence microscopy was next used to test for the effects of the induction of LOX-PP on the localization of β-catenin using H1299-EV and clone 8 for analysis. In the control EV lung cancer cells, little of the β-catenin was seen on the cell membrane and at cell-cell contacts (Fig. 7B). Treatment with Dox had no detectable effect on this pattern (Fig. 7B). Untreated H1299 clone 8 cells showed a higher degree of membrane accumulation of β-catenin, which likely relates to the low level of LOX-PP expression in the absence of Dox due to leakiness of vector expression in these cells (46). Upon the induction of LOX-PP expression, the level of β-catenin in the cytoplasm decreased markedly and a substantial increase in the accumulation of β-catenin at the plasma membrane was observed (Fig. 7B). To extend the findings to additional clones, clone 3 and clone 5 and control EV cells were treated with Dox and similarly analyzed. Both clones showed higher levels of membrane β-catenin than EV control cells did (Fig. 7C). The effects of LOX-PP expression on the levels of β-catenin in the nuclear fraction in these clones was further monitored using immunoblotting. LOX-PP expression led to decreased levels of β-catenin in the nuclei of the lung cancer cells (Fig. 7D). The use of lamin B confirmed essentially equal loading. The results of three independent experiments were quantified, and the normalized nuclear β-catenin levels in clones 3 and 5 had decreased an average of 0.29 and 0.56, respectively, relative to the control levels. Thus, LOX-PP results in relocalization of β-catenin from the nucleus to the cell membrane at sites of cell-cell contact.

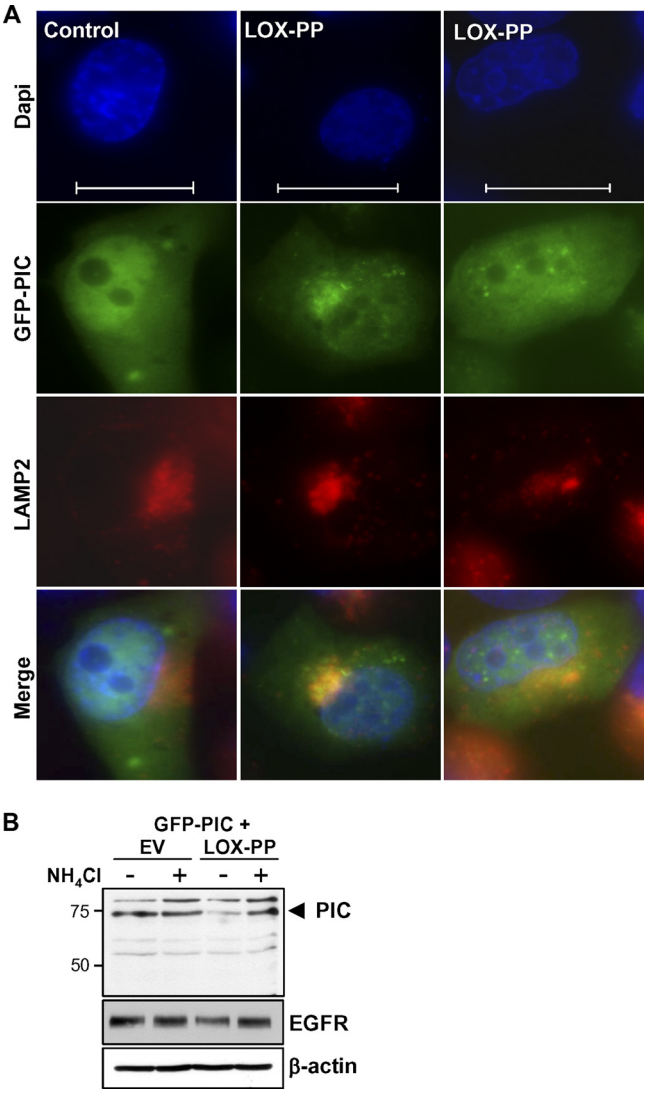

FIG. 6. LOX-PP leads to relocalization to the lysosome and degradation of PIC. (A) H1299 cells were cotransfected with GFP-PIC and a V5-tagged LOX-PP construct or EV DNA, as control. For lysosome staining, a LAMP2 antibody and anti-mouse Alexa Fluor 555-IgG antibody were used. Nuclei were labeled with DAPI (blue). Individual and merged images are shown. Fluorescence microscopy was performed as described in the Fig. 5 legend. Bars = 60 μm. (B) H1299 cells were transfected overnight with vectors expressing GFP-PIC with either LOX-PP or EV DNA and treated with 20 mM NH_4Cl, a lysosomal inhibitor, for 4 h. Whole-cell extracts were prepared and subjected to immunoblotting for PIC, EGFR, and β-actin, as indicated.

LOX-PP inhibits β-catenin transcriptional activity in lung cancer cells. The observed relocalization of β-catenin leads to the prediction that LOX-PP expression will result in decreased β-catenin-driven transcriptional activity. To evaluate functional β-catenin-mediated transactivation, we used the TOP-Flash reporter that harbors six LEF-1/TCF-binding sites (4). Parallel transfections were performed using pFOP, containing all of the regulatory elements of the pTOP-Flash plasmid except that the TCF response motifs contain mutations that prevent its functional activation by TCF. H1299 cells were

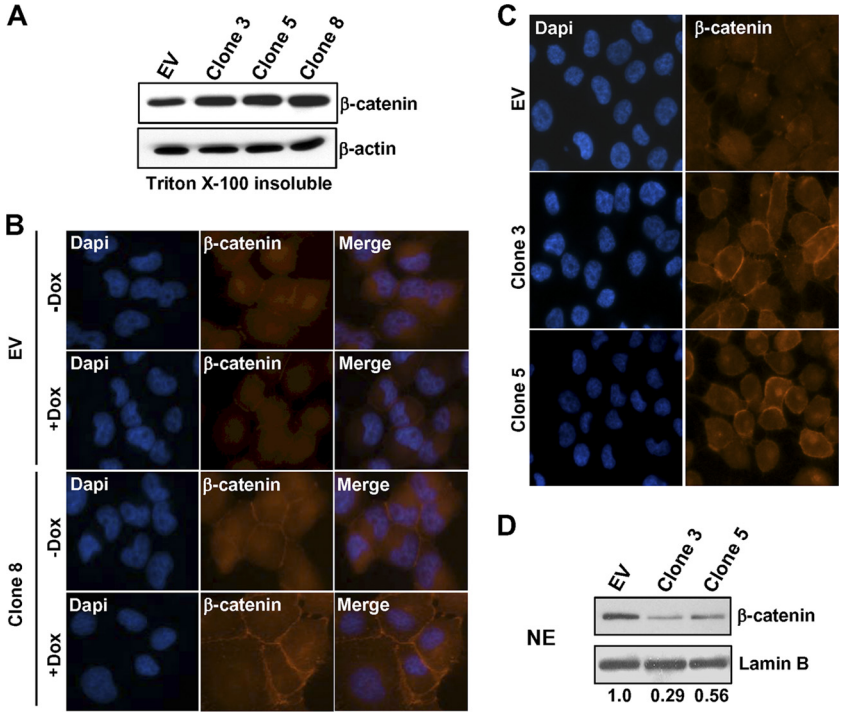

FIG. 7. LOX-PP promotes β-catenin redistribution from the nucleus to the plasma membrane. (A) Control (EV) and LOX-PP-expressing clones 3, 5, and 8 were incubated in the presence of Dox for 48 h. The Triton X-100-insoluble membrane fraction was prepared and subjected to immunoblotting for β-catenin and for β-actin as a loading control. (B) Control (EV) or clone 8 H1299 lung cancer cells were incubated in the absence (−Dox) or presence (+Dox) of Dox for 48 h. For β-catenin staining, a primary mouse β-catenin antibody and a secondary anti-mouse Alexa Fluor 594 IgG antibody (red) were used. Nuclei were labeled with DAPI (blue). Fluorescence microscopy was performed on a Zeiss Axiovert 200 M microscope, and images taken using a 40× objective. Individual and merged images are shown. (C) Control (EV) or LOX-PP-expressing clones 3 and 5 were incubated in the presence of Dox for 48 h and subjected to fluorescence microscopy as described for panel B. (D) Control (EV) or LOX-PP-expressing clones 3 and 5 were incubated in the presence of Dox for 48 h, and nuclear extracts (NE) were prepared and subjected to immunoblotting for β-catenin and for lamin B, which confirmed essentially equal loading. This experiment and blots from two replicate experiments were scanned, and the changes relative to the results for the control EV, set at 1.0, are presented below.

transfected with pTOP or pFOP and a control EV vector or a LOX-PP expression plasmid in combination with a *Renilla* luciferase plasmid as an internal control. The expression of LOX-PP in H1299 lung cancer cells reduced LEF-1/TCF-driven luciferase activity by approximately 72% ($P = 0.0067$) (Fig. 8A). A similar reduction was obtained in the A549 lung cancer cell line (59.2% [$P = 0.009$], data not shown). Thus, LOX-PP reduces overall β-catenin transcriptional activity.

Several identified targets of β-catenin transcriptional activity are expressed in lung cancer cells, including c-*MYC*, *EGFR*, and *FRA-1* (8, 18, 23). To test whether LOX-PP reduces the expression of these genes, real-time PCR analysis was performed (Fig. 8B). Substantial decreases were observed in mRNA expression from these genes upon Dox-mediated induction of LOX-PP in H1299 clones 3 and 5 versus the levels of expression in EV DNA cells. Next, Western blotting was performed on whole-cell extracts of the H1299 EV control or LOX-PP clones 3 and 5 that had been incubated in the presence of Dox for 48 h. Compared to the levels in the control EV H1299 cells, the levels of c-MYC, Fra-1, and EGFR proteins were substantially reduced in the LOX-PP-expressing clones (Fig. 8C). Together, these findings indicate that the relocalization of the β-catenin protein induced by LOX-PP expression leads to an overall reduction in the expression of β-catenin-dependent genes.

DISCUSSION

Here, LOX-PP was shown to interact with the phosphatase domains of the multifunctional protein RPTP-κ and decrease the relative level of its PIC isoform that chaperones β-catenin to the nucleus, thereby decreasing β-catenin transcriptional activity in lung cancer cells. Conversely, LOX-PP increased the relative level of the RPTP-κ P isoform, which functions to stabilize β-catenin on the cell surface, leading to decreased lung cancer cell migration. RPTP-κ was identified as a novel LOX-PP-associating protein using a yeast two-hybrid assay. The clone we isolated encoded the phosphatase domains of RPTP-κ, common to both the P and PIC isoforms. The significance of the interaction with LOX-PP was studied in lung cancer cells, which express high levels of the RPTP-κ protein. We found that the nuclear levels of PIC were reduced in H1299 lung cancer cells in the presence of LOX-PP as judged by immunofluorescence analysis of cells coexpressing GFP-PIC and a V5-tagged LOX-PP and by Western blot analysis of nuclear fractions of LOX-PP-expressing and control H1299 lung cancer cell clones. Commensurately, LOX-PP decreased β-catenin-mediated transcriptional activity in H1299 and A549 lung cancer cells, as judged by reduced luciferase reporter activity. LOX-PP also reduced the levels of mRNA and protein expression of the β-catenin-dependent genes c-*MYC*, *FRA-1*,

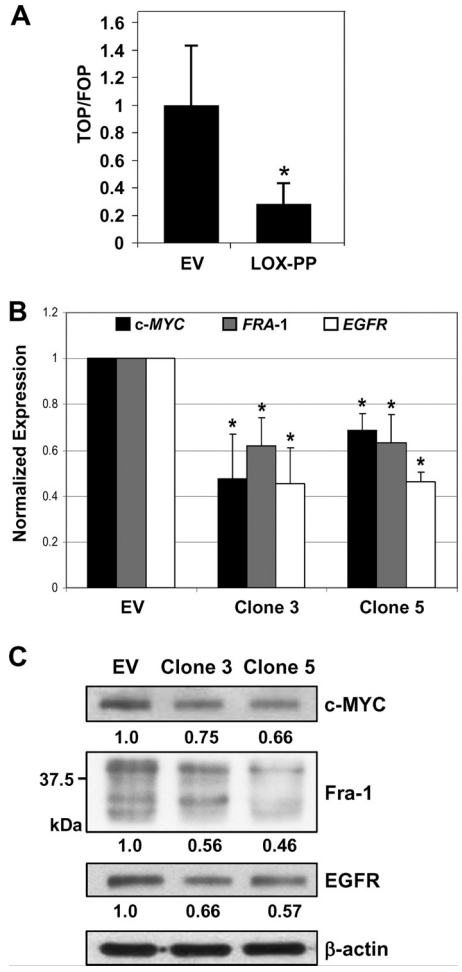

FIG. 8. LOX-PP inhibits β-catenin transcriptional activity. (A) H1299 cells were transfected, in triplicate, with 1 μg of either control EV DNA or LOX-PP expression plasmid in the presence of 500 ng of either pTOP-Flash or pFOP-Flash TCF reporter plasmids and 10 ng of a *Renilla* luciferase plasmid as an internal control for transfection. Luciferase activities are shown as the ratio of TOP/FOP activities. The assay was repeated three times in triplicate; values for TOP/FOP were normalized to 1 for the EV control, and results are presented with plus-minus standard deviations. Significance was determined by using Student's *t* test. *, *P* value = 0.0067. (B) Real-time PCR analysis of the expression of c-*MYC*, *FRA-1*, and *EGFR* mRNA levels in control (EV) or LOX-PP-expressing clones 3 and 5 in a 96-well plate was performed using a Roche Light Cycler 480II. All reactions were performed three times in triplicate. Significance was determined using Student's *t* test. *, significant difference. *P* values for c-*MYC* were 0.029 and 0.0016 for clones 3 and 5, respectively; *P* values for *FRA-1* were 0.0058 and 0.048 for clones 3 and 5, respectively; and *P* values for *EGFR* were 0.0038 and 0.0007 for clones 3 and 5, respectively. (C) Whole-cell extracts were prepared from control (EV) or LOX-PP-expressing clones 3 and 5 and subjected to immunoblotting for c-MYC, Fra-1, and EGFR and for β-actin, which confirmed equal loading. The values for the extent of reduced expression, derived by densitometric analysis of the data in this and a duplicate blot, are given below each lane.

and *EGFR*. Interestingly, we found that in the presence of LOX-PP, GFP-PIC colocalized with lysosomal proteins, suggesting that the decreased levels and nuclear accumulation might be due to turnover. Consistently, treatment of cells with the lysosome inhibitor ammonium chloride reversed the depletion of GFP-PIC, confirming our hypothesis. Notably, results from our group and those of Shames et al. have shown that *LOX* gene expression is greatly reduced in lung cancer cells and would be unable to influence PIC isoform stability or processing (42, 46). We find that with partial knockdown of LOX-PP, the levels of the P subunit were decreased, but changes in the total levels of PIC were not detected. As β-catenin–TCF–LEF complexes are key effectors of oncogenic signaling pathways, this study elucidates a novel mechanism of tumor suppressor activity of LOX-PP in lung cancer cells.

RPTP-κ is a member of the receptor-like protein tyrosine phosphatase family that is involved in the regulation of cell contact formation (9). We focused on RPTP-κ due to the accumulating evidence of its role as a tumor suppressor gene that is often silenced or deleted in human tumors (34). The *RPTP*κ gene maps to a putative tumor suppressor gene region in chromosome 6 and is a potential deletion target in a variety of tumors, including pancreatic cancer, breast cancer, ovarian carcinoma, melanoma, leukemia, non-Hodgkin lymphoma, and primary central nervous system lymphomas (7, 34, 48). In addition, RPTP-κ is reported to be upregulated by TGF-β treatment in primary human keratinocytes and is involved in the negative regulation of signal pathways induced by receptor tyrosine kinases (34, 47).

Importantly, RPTP-κ has recently emerged as a novel regulator of β-catenin function in mammalian cells, including lung cancer cells (9). The P subunit maintains β-catenin at the cell surface and represses its transcriptional activity, whereas the PIC isoform functions to move β-catenin to the nucleus and serves as an activator. Consistently, the levels of the membrane-associated P isoform were lowest in the highly metastatic A549 and H1299 cells of the human lung cancer lines examined. While mutations in the β-catenin gene *CTNNB1* and *APC* are seen frequently in colon cancer, they are quite rare in lung cancer (14, 29), whereas activating Ras and EGFR mutations are frequently seen in lung cancer (39, 43). Notably, Nguyen et al. observed gene expression signatures indicative of hyperactive Wnt/TCF signaling associated with high rates of relapse of lung cancer and metastases to distant sites, including the brain and bone (33). Furthermore, they found that LEF1 was a critical mediator of brain and bone metastases by lung adenocarcinoma lines. Notably, the interaction of LOX-PP and RPTP-κ and the inhibitory role of LOX-PP on TCF/LEF-mediated transcriptional activities have recently been extended to breast cancer (N. Sánchez-Morgan, unpublished observations). Nuclear accumulation of β-catenin is also recognized as an important marker for fibroproliferative disorders of the lung (13), suggesting that our findings have significant clinical ramifications.

RPTP-κ was among several clones of putative LOX-PP-associated proteins isolated in the yeast two-hybrid assay. Interestingly, LOX-PP has been reported to localize to multiple cellular locations (extracellular matrix, Golgi complex, and lysosome in the cytoplasm, as well as perinuclear and potentially nuclear sites), suggesting that it might be exerting its tumor suppressor activity through different mechanisms. In differentiating osteoblasts, LOX-PP localizes to the cytoplasm where it associates with the microtubule network, while in proliferating osteoblasts, LOX-PP has been detected in the Golgi complex and endoplasmic reticulum (15). In lung cancer

cells, we found that LOX-PP is primarily in the cytoplasm (with some diffuse nuclear staining) and accumulates in the perinuclear region in the *trans*-Golgi network (Fig. 5 and data not shown). Consistent with its diverse cellular localization, multiple mechanisms of action have been reported recently for LOX-PP action. For example, our group has shown that rLOX-PP protein inhibits Ras signaling in prostate cancer cells in part by reducing FGF signaling (36). Similarly, a role for LOX-PP as an inhibitor of axonal growth by Purkinje cells has been reported to be due to its ability to inhibit the activity of the NF-κB p65 subunit (26). Moreover, we have also recently found that LOX-PP can interact directly with the chaperone protein Hsp70 and its binding partner c-Raf, thereby reducing Ras signaling via the Erk axis node (40a). In summary, in this study, a novel association of LOX-PP with the receptor-type tyrosine phosphatase RPTP-κ is identified. This interaction leads to an inhibition of β-catenin function in lung cancer cells, which represents a new mechanism of action for the tumor suppressor LOX-PP.

ACKNOWLEDGMENTS

We thank Axel Ullrich, Gary Fisher, Isabel Dominguez, and T. Akagi for generously providing antibody reagents, cloned DNAs, and viral vectors and Zhi-Xiong Jim Xiao, Hasmeena Kathuria, and Alvin Malkinson for cell lines. We gratefully acknowledge C. O'Neill for assistance with the migration assays.

These studies were supported by NIH grants RO1 CA082742, RO1 CA143108, and PO1 ES011624.

REFERENCES

1. **Akiri, G., et al.** 2009. Wnt pathway aberrations including autocrine Wnt activation occur at high frequency in human non-small-cell lung carcinoma. Oncogene **28:**2163–2172.
2. **Anders, L., et al.** 2006. Furin-, ADAM 10-, and gamma-secretase-mediated cleavage of a receptor tyrosine phosphatase and regulation of beta-catenin's transcriptional activity. Mol. Cell. Biol. **26:**3917–3934.
3. **Bouez, C., et al.** 2006. The lysyl oxidase LOX is absent in basal and squamous cell carcinomas and its knockdown induces an invading phenotype in a skin equivalent model. Clin. Cancer Res. **12:**1463–1469.
4. **Chitalia, V. C., et al.** 2008. Jade-1 inhibits Wnt signalling by ubiquitylating beta-catenin and mediates Wnt pathway inhibition by pVHL. Nat. Cell Biol. **10:**1208–1216.
5. **Contente, S., K. Kenyon, D. Rimoldi, and R. M. Friedman.** 1990. Expression of gene rrg is associated with reversion of NIH 3T3 transformed by LTR-c-H-ras. Science **249:**796–798.
6. **Contente, S., K. Kenyon, P. Sriraman, S. Subramanyan, and R. M. Friedman.** 1999. Epigenetic inhibition of lysyl oxidase transcription after transformation by ras oncogene. Mol. Cell. Biochem. **194:**79–91.
7. **Eswaran, J., J. E. Debreczeni, E. Longman, A. J. Barr, and S. Knapp.** 2006. The crystal structure of human receptor protein tyrosine phosphatase kappa phosphatase domain 1. Protein Sci. **15:**1500–1505.
8. **Fogelgren, B., et al.** 2005. Cellular fibronectin binds to lysyl oxidase with high affinity and is critical for its proteolytic activation. J. Biol. Chem. **280:**24690–24697.
9. **Fuchs, M., T. Muller, M. M. Lerch, and A. Ullrich.** 1996. Association of human protein-tyrosine phosphatase kappa with members of the armadillo family. J. Biol. Chem. **271:**16712–16719.
10. **Gavert, N., and A. Ben-Ze'ev.** 2007. Beta-catenin signaling in biological control and cancer. J. Cell. Biochem. **102:**820–828.
11. **Gebbink, M. F., et al.** 1995. Cell surface expression of receptor protein tyrosine phosphatase RPTP mu is regulated by cell-cell contact. J. Cell Biol. **131:**251–260.
12. **Giampuzzi, M., et al.** 2000. Lysyl oxidase activates the transcription activity of human collagen III promoter. Possible involvement of Ku antigen. J. Biol. Chem. **275:**36341–36349.
13. **Gosens, R., et al.** 2010. De novo synthesis of {beta}-catenin via H-Ras and MEK regulates airway smooth muscle growth. FASEB J. **24:**757–768.
14. **Gotz, R.** 2008. Inter-cellular adhesion disruption and the RAS/RAF and beta-catenin signalling in lung cancer progression. Cancer Cell Int. **8:**7.
15. **Guo, Y., N. Pischon, A. H. Palamakumbura, and P. C. Trackman.** 2007. Intracellular distribution of the lysyl oxidase propeptide in osteoblastic cells. Am. J. Physiol. Cell Physiol. **292:**C2095–C3102.
16. **Hajnal, A., R. Klemenz, and R. Schafer.** 1993. Up-regulation of lysyl oxidase in spontaneous revertants of H-ras-transformed rat fibroblasts. Cancer Res. **53:**4670–4675.
17. **Hamalainen, E. R., et al.** 1995. Quantitative PCR of lysyl oxidase mRNA in malignantly transformed human cell lines demonstrates that their low lysyl oxidase activity is due to low quantities of its mRNA and low levels of transcription of the respective gene. J. Biol. Chem. **270:**21590–21593.
18. **He, T. C., et al.** 1998. Identification of c-MYC as a target of the APC pathway. Science **281:**1509–1512.
19. **Jeay, S., S. Pianetti, H. M. Kagan, and G. E. Sonenshein.** 2003. Lysyl oxidase inhibits ras-mediated transformation by preventing activation of NF-kappa B. Mol. Cell. Biol. **23:**2251–2263.
20. **Jiang, Y. P., et al.** 1993. Cloning and characterization of R-PTP-kappa, a new member of the receptor protein tyrosine phosphatase family with a proteolytically cleaved cellular adhesion molecule-like extracellular region. Mol. Cell. Biol. **13:**2942–2951.
21. **Kaneda, A., et al.** 2004. Lysyl oxidase is a tumor suppressor gene inactivated by methylation and loss of heterozygosity in human gastric cancers. Cancer Res. **64:**6410–6415.
22. **Kenyon, K., et al.** 1991. Lysyl oxidase and rrg mRNA. Science **253:**802.
23. **Kirschmann, D. A., E. A. Seftor, D. R. Nieva, E. A. Mariano, and M. J. Hendrix.** 1999. Differentially expressed genes associated with the metastatic phenotype in breast cancer. Breast Cancer Res. Treat. **55:**127–136.
24. **Krzyzosiak, W. J., N. Shindo-Okada, H. Teshima, K. Nakajima, and S. Nishimura.** 1992. Isolation of genes specifically expressed in flat revertant cells derived from activated ras-transformed NIH 3T3 cells by treatment with azatyrosine. Proc. Natl. Acad. Sci. U. S. A. **89:**4879–4883.
25. **Kuivaniemi, H., R. M. Korhonen, A. Vaheri, and K. I. Kivirikko.** 1986. Deficient production of lysyl oxidase in cultures of malignantly transformed human cells. FEBS Lett. **195:**261–264.
26. **Li, J., et al.** 2010. Nna1 mediates Purkinje cell dendritic development via lysyl oxidase propeptide and NF-kappaB signaling. Neuron **68:**45–60.
27. **Lucero, H. A., and H. M. Kagan.** 2006. Lysyl oxidase: an oxidative enzyme and effector of cell function. Cell. Mol. Life Sci. **63:**2304–2316.
28. **Mann, B., et al.** 1999. Target genes of beta-catenin-T cell-factor/lymphoid-enhancer-factor signaling in human colorectal carcinomas. Proc. Natl. Acad. Sci. U. S. A. **96:**1603–1608.
29. **Mazieres, J., B. He, L. You, Z. Xu, and D. M. Jablons.** 2005. Wnt signaling in lung cancer. Cancer Lett. **222:**1–10.
30. **Min, C., et al.** 2007. The tumor suppressor activity of the lysyl oxidase propeptide reverses the invasive phenotype of Her-2/neu-driven breast cancer. Cancer Res. **67:**1105–1112.
31. **Min, C., et al.** 2009. A loss-of-function polymorphism in the propeptide domain of the LOX gene and breast cancer. Cancer Res. **69:**6685–6693.
32. **Monteiro, A. N., A. August, and H. Hanafusa.** 1996. Evidence for a transcriptional activation function of BRCA1 C-terminal region. Proc. Natl. Acad. Sci. U. S. A. **93:**13595–13599.
33. **Nguyen, D. X., et al.** 2009. WNT/TCF signaling through LEF1 and HOXB9 mediates lung adenocarcinoma metastasis. Cell **138:**51–62.
34. **Novellino, L., et al.** 2008. PTPRK negatively regulates transcriptional activity of wild type and mutated oncogenic beta-catenin and affects membrane distribution of beta-catenin/E-cadherin complexes in cancer cells. Cell. Signal. **20:**872–883.
35. **Palamakumbura, A. H., et al.** 2004. The propeptide domain of lysyl oxidase induces phenotypic reversion of ras-transformed cells. J. Biol. Chem. **279:**40593–40600.
36. **Palamakumbura, A. H., et al.** 2009. Lysyl oxidase propeptide inhibits prostate cancer cell growth by mechanisms that target FGF-2-cell binding and signaling. Oncogene **28:**3390–3400.
37. **Perego, C., C. Vanoni, S. Massari, R. Longhi, and G. Pietrini.** 2000. Mammalian LIN-7 PDZ proteins associate with beta-catenin at the cell-cell junctions of epithelia and neurons. EMBO J. **19:**3978–3989.
38. **Ren, C., G. Yang, T. L. Timme, T. M. Wheeler, and T. C. Thompson.** 1998. Reduced lysyl oxidase mRNA levels in experimental and human prostate cancer. Cancer Res. **58:**1285–1290.
39. **Rodenhuis, S., et al.** 1988. Incidence and possible clinical significance of K-ras oncogene activation in adenocarcinoma of the human lung. Cancer Res. **48:**5738–5741.
40. **Sap, J., Y. P. Jiang, D. Friedlander, M. Grumet, and J. Schlessinger.** 1994. Receptor tyrosine phosphatase R-PTP-kappa mediates homophilic binding. Mol. Cell. Biol. **14:**1–9.

40a. **Sato, S., et al.** 2011. The Ras signaling inhibitor LOX-PP interacts with Hsp70 and c-Raf to reduce Erk activation and transformed phenotype of breast cancer cells. Mol. Cell. Biol. **31:**2683–2695.

41. **Seibel, N. M., J. Eljouni, M. M. Nalaskowski, and W. Hampe.** 2007. Nuclear localization of enhanced green fluorescent protein homomultimers. Anal. Biochem. **368:**95–99.
42. **Shames, D. S., et al.** 2006. A genome-wide screen for promoter methylation in lung cancer identifies novel methylation markers for multiple malignancies. PLoS Med. **3:**e486.
43. **Sharma, S. V., D. W. Bell, J. Settleman, and D. A. Haber.** 2007. Epidermal

growth factor receptor mutations in lung cancer. Nat. Rev. Cancer **7:**169–181.
44. **Tan, X., et al.** 2005. Epidermal growth factor receptor: a novel target of the Wnt/beta-catenin pathway in liver. Gastroenterology **129:**285–302.
45. **Vora, S. R., et al.** 2010. Lysyl oxidase propeptide inhibits FGF-2-induced signaling and proliferation of osteoblasts. J. Biol. Chem. **285:**7384–7393.
46. **Wu, M., et al.** 2007. Repression of BCL2 by the tumor suppressor activity of the lysyl oxidase propeptide inhibits transformed phenotype of lung and pancreatic cancer cells. Cancer Res. **67:**6278–6285.
47. **Xu, Y., et al.** 2010. Receptor type protein tyrosine phosphatase-kappa mediates cross-talk between transforming growth factor-beta and epidermal growth factor receptor signaling pathways in human keratinocytes. Mol. Biol. Cell **21:**29–35.
48. **Yang, Y., et al.** 1997. Molecular cloning and chromosomal localization of a human gene homologous to the murine R-PTP-kappa, a receptor-type protein tyrosine phosphatase. Gene **186:**77–82.
49. **Zhao, Y., et al.** 2009. The lysyl oxidase pro-peptide attenuates fibronectin-mediated activation of focal adhesion kinase and p130Cas in breast cancer cells. J. Biol. Chem. **284:**1385–1393.
50. **Zondag, G. C., et al.** 1995. Homophilic interactions mediated by receptor tyrosine phosphatases mu and kappa. A critical role for the novel extracellular MAM domain. J. Biol. Chem. **270:**14247–14250.